Investigating a Non-Invasive Method for Determining Muscle Fiber Composition

by

Laura Treers

Submitted to the
Department of Mechanical Engineering
in Partial Fulfillment of the Requirements for the Degree of

Bachelor of Science in Mechanical Engineering

at the

Massachusetts Institute of Technology

June 2018

Signature of Author: Signature redacted
Department of Mechanical Engineering
May 14, 2018

Certified by: Signature redacted
Anette Hosoi
Professor of Mechanical Engineering
Thesis Supervisor

Accepted by: Signature redacted
Rohit Karnik
Professor of Mechanical Engineering
Undergraduate Officer

Investigating a Non-Invasive Method for Determining Muscle Fiber Composition

by

Laura Treers

Submitted to the Department of Mechanical Engineering
on May 14, 2018 in Partial Fulfillment of the
Requirements for the Degree of

Bachelor of Science in Mechanical Engineering

ABSTRACT

This study aims to explore a new method for analysis of muscle fiber type, using data collected from weightlifts on a leg press. A dynamic muscle model is developed, which utilizes the Descherevskii kinetic theory in combination with a muscle "matrix" model to predict net muscle contraction forces and velocities as a function of fiber type. These relationships are integrated into a dynamic model for lifting a weight, allowing for the derivation of joint trajectories in time, from the molecular properties of muscle. The model-predicted velocity trajectories for the lift are compared with curves obtained experimentally from weightlifting trials. Longer lifts with slower peak velocities indicate higher ratios of slow-twitch fibers, and shorter lifts with greater peak velocities indicate higher ratios of fast-twitch fibers. This idea is supported by both the model results and in experimental trends. With further refinement of experimental protocols, the leg press test has the potential to be a powerful training tool for athletes—both to compare their muscle makeup with other athletes, and to track their own progress over the course of their training.

Thesis Supervisor: Anette Hosoi
Title: Professor of Mechanical Engineering

ACKNOWLEDGEMENTS

In the completion of this thesis project, there were many important people without whom these results wouldn't have been realized. Thank you first to my thesis advisor Anette (Peko) Hosoi, for the positive inspiration, and for guiding me through all aspects of the project. I would also like to thank the members of the Hatsopoulos Microfluids Lab, particularly grad student Sarah Fay, who helped me with my modeling efforts and troubleshooting various parts of the project, from start to finish.

Also, I'd like to recognize the students of Team Red Bull in the MIT Sports Tech Class 2.S983 for working alongside me to design and create a device for the Red Bull training facility. Their device will create output velocity profiles for athletes that allow the model I've worked on to estimate fiber composition. In other words, their work makes my work become a reality.

I'd like to especially recognize the amazing work of our research partners at LadHyX (Laboratoire Hydrodynamique de L'Ecole Polytechnique) in Palaiseau, France. The work on muscle fiber biomechanics by Caroline Cohen and Christophe Clanet at LadHyX provided the basis for my work, and they also provided significant guidance over the course of my research process. Thanks very much to the folks at LadHyX for being extremely kind and supportive of my endeavors, and for hosting me at Ecole Polytechnique for the month of January to conduct research in their lab.

Table of Contents

List of Figures

List of Tables

1. Introduction

The purpose of this study is to explore the possibility of a non-invasive method to determine muscle fiber type composition (slow vs. fast twitch) in human muscle. A mathematical model for muscle contraction is introduced, which begins at the molecular level (sliding filament model) and is extrapolated to trajectories of the limbs using joint kinematic and dynamic relations. With this model, it is possible to predict the output velocity trajectories during a weighlift, with knowledge of the athlete's weight, limb length, and fast twitch fiber ratio "R." The model output trajectories are compared to data collected experimentally for weightlifting trials, to explore the potential for a one-rep max leg press to be a non-invasive indicator of muscle fiber type composition.

1.1 Slow vs. Fast Twitch Fibers

As commonly accepted in muscle physiology, there exist at least two distinct types of muscle fibers, referred to most often as slow-twitch and fast-twitch. These names reference the twitch response time of the muscle fibers to triggering by a motoneuron action potential. Functionally, Slow Twitch (or Type I/ Slow Oxidative) fibers are characterized by slower contraction velocities and higher resistance to fatigue. Conversely, Fast Twitch (or Type II) fibers can be characterized by faster contraction velocities, but fatigue much more quickly than slow twitch fibers. In many cases, Type II fibers are characterized into two subcategories—Type IIB (Fast fatiguable, FR) are extremely sensitive to fatigue and reserved for high output anaerobic efforts, while Type IIA (Fatigue Resistant, FR) represent an intermediate fatigue resistance, with a significantly faster contraction time than Type I fibers [1].

1.1.1 Muscle Physiology

On the cellular level, muscles are divided into long strands of muscle fibers, which are made up of strands known as myofibrils, the cellular unit of muscle tissue. Myofibrils are composed of strands of myofilaments, which contain sarcomeres, the basic functional unit of force production. Sarcomeres, in turn, contain bundles of thick and thin filaments, comprised of myosin and actin molecules, respectively. Actin and myosin are the active units of force production, which by "sliding" relative to one another, create a tension actuator [2]. This action is described by the sliding filament model, which is discussed in the introduction of a biomechanical model in further sections of the paper.

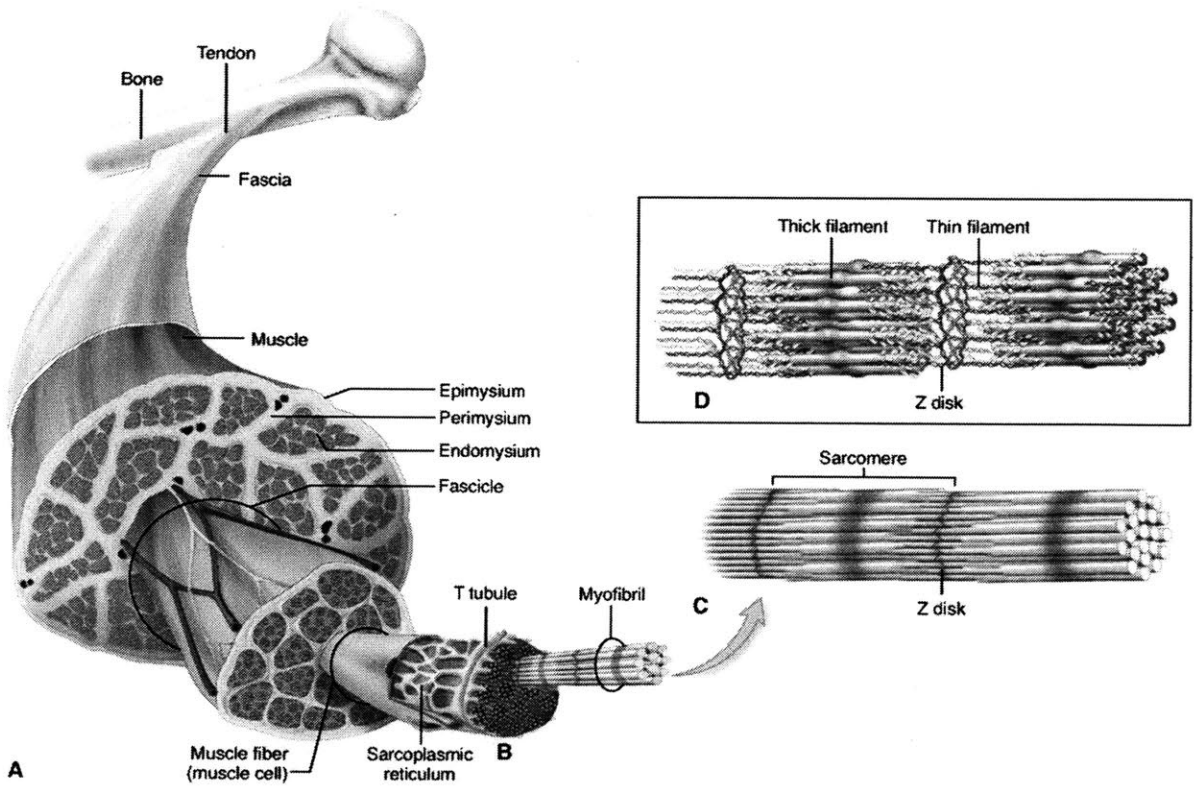

Figure 1: A diagram of the breakdown of skeletal muscle organization, from full muscle to muscle fiber (myofibril) to actin & myosin molecules (here, labeled thick & thin filaments). Image reproduced from [3], "Physiology of the Muscular System," *Basicmedical Key*

From a physiological standpoint, the discrepancy between slow and fast-twitch response lies at the level of the myofiber (an individual muscle cell or bundle of sarcomeres), and is caused by a difference in the release rate of calcium by the sarcoplasmic reticulum in the muscle cells, and the rate at which enzymes work to break down ATP in the myosin heads of contractile proteins. In fast-twitch fibers, the rates of these two processes are greater, leading to greater contraction speeds. Structurally, fast twitch fibers are triggered by larger motoneuron axons, and have larger fiber diameters in comparison with slow twitch fibers. Slow twitch fibers have a high mitochondrial content and blood supply, which gives them a characteristic red color and high resistance to fatigue. While fast twitch fibers, on the other hand, can produce much higher tetanic tensions, they have a relatively smaller blood supply and mitochondrial content, leaving them more prone to fast fatigue and giving them their white appearance [4].

1.1.2 Significance of Fiber Type to Athletes

It is commonly believed that all people lie on a "spectrum" ranging from mostly slow twitch to mostly fast twitch fibers. Those whose muscles are primarily slow twitch perform better in longer, more sustained endurance efforts, but have more trouble with short-duration, explosive efforts. Similarly, those who have primarily fast-twitch fibers can perform better in short, high-intensity bursts of power, but cannot maintain efforts for longer periods of time.

Moreover, in some sports it is beneficial to have a particular fiber makeup. For example, marathon runners or endurance cyclists likely prefer to be almost entirely slow-twitch fibers, to be able to run or ride for long hours without sign of muscle fatigue. Conversely, track sprinters, for example, prefer to have almost entirely fast-twitch fibers, to produce maximal forces at the expense of quick muscle fatigue. In most sports however, the "desired" ratio lies on a spectrum

between these two extremes, and will depend on the types and durations of muscular efforts involved.

1.2 Methods for Determining Fiber Type

Today, there exist very few methods for determining athlete fiber type. They are either costly and invasive, or are indirect methods that provide only an approximate fiber ratio value. Atheletes wishing to know their exact fiber type ratio can undergo a muscle biopsy, in which a small piece of the person's muscle is removed for examination under a microscope. The number of slow vs. fast fibers are visible and countable, which allows for a relatively accurate ratio measurement for the sampled muscle. To measure this ratio in other muscles, biopsy samples would be needed from each different desired muscle group.

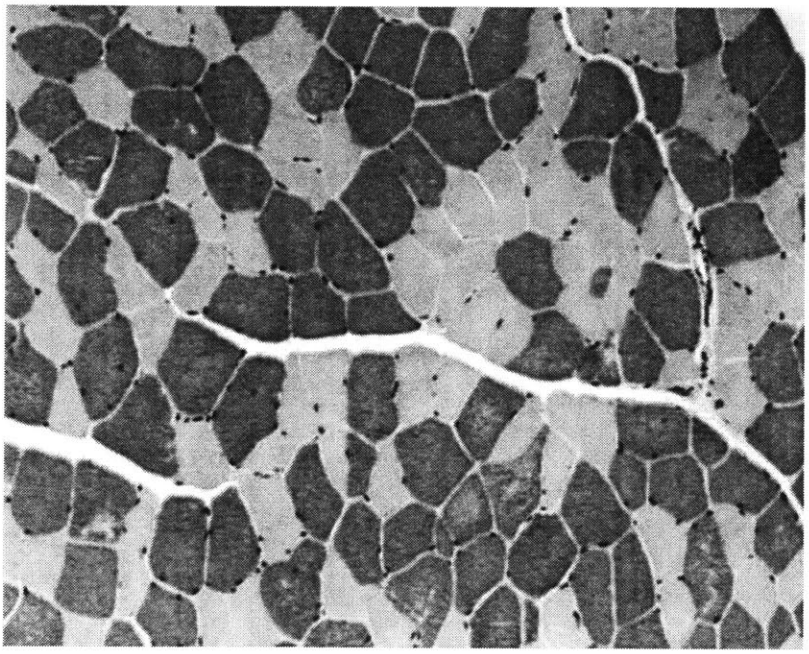

Figure 2: A sample of a human skeletal muscle cross-section, such as that examined in a fiber type biopsy test. Type I fibers are clearly a darker red than the rest, while Type II fibers appear white or pink-tinged. Image reproduced from [5], E. Sierra, et al, "Muscular senescence in cetaceans: adaptation towards a slow muscle fibre phenotype," *Scientific Reports*

Another method is also currently in use by athletic trainers and coaches, which is noninvasive but a coarse approximation. It requires the athlete to determine the maximum weight they can lift for a given muscle group, and do as many repetitions as possible at 80% of their maximum weight. Greater than 12 repetitions indicates a greater than 50% distribution of slow-twitch fibers, less than 7 repetitions indicates >50% fast-twitch fibers, and a result of 7-12 repetitions indicates that the athlete's fiber type ratio is approximately evenly split between the two fiber types [1].

2. Background

2.1 Mechanism of Muscle Force Production

2.1.1 The Actomyosin Cycle

The coined "Actomyosin cycle" is the name for the cycle of molecular interaction in skeletal muscle that results in force production. It is described by the "sliding filament hypothesis," in which the sliding motion between myosin and actin molecules is repeated, leading to the formation of tension in the muscle. This actomyosin crossbridge cycle can be described as follows: In the absence of ATP (adenosine tri-phosphate), myosin heads bind to sites on the actin filaments. When ATP is present, it reacts with the myosin heads, causing them to detach and rotate to a new position, entering a high-energy state. The presence of Ca 2+ ions allows the myosin heads to re-attach to the actin and rotate back to their original configuration. This cycle is repeated and the myosin heads re-attach at new binding sites, leading the myosin heads to continually "climb" along the actin filament surface [6]. The actin and myosin slide relative to one another in discrete steps described by each cycle of attachment and detachment, leading to the descriptor "sliding filaments." This process is illustrated in Figure 3.

Skeletal muscle acts like a tension actuator, meaning that changes in muscle length are closely related to the production of muscle force. Each "power stroke" of a myosin head in the sliding filament model creates a discrete amount of force, as well as a discrete change in the length of the fiber. This assumption holds true for traditional muscle contractions where force is generated exceeding the opposing load, ie. concentric contractions. In eccentric contractions, the muscle works to oppose an applied force and joints decelerate, while in isometric contractions the muscle length is assumed to be fixed and forces are generated or opposed. This study is concerned with concentric contractions (like those seen in weightlifting), which allow for the development of a well-defined force-length relationship, and a relationship between force production in the muscle and the number of active myosin heads.

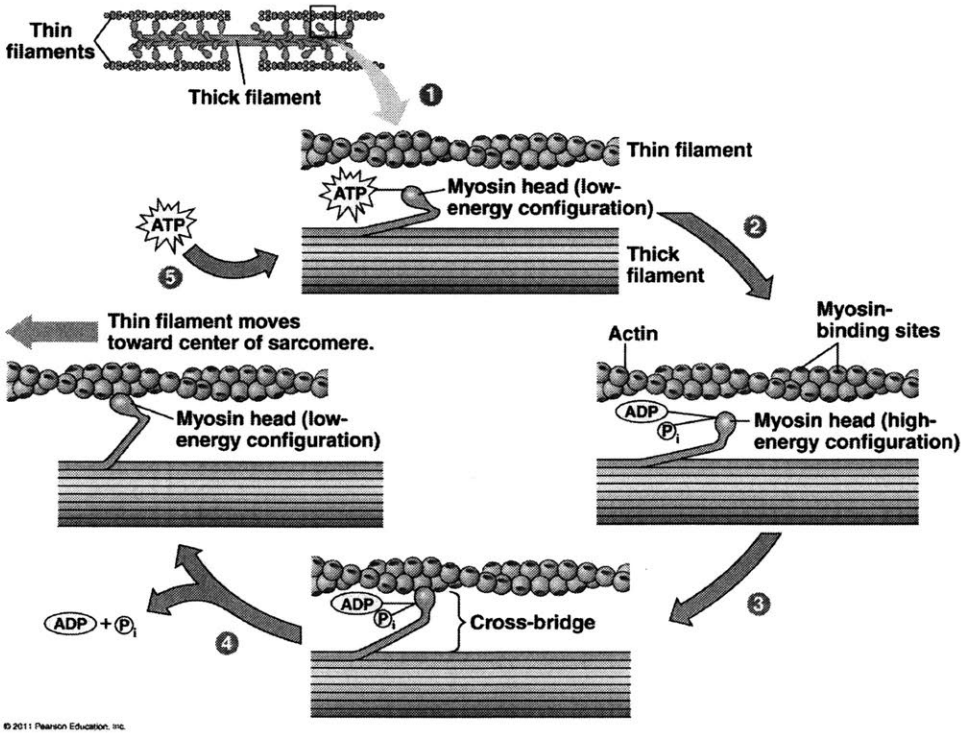

Figure 3: The Actomyosin cross-bridge cycle in skeletal muscle. The five steps depicted here represent 1) Addition of ATP in a low-energy configuration 2) Hydrolysis of ATP to ADP, leading to a high-energy configuration 3) Attachment of myosin head to binding site on the actin filament 4) Myosin "power stroke" returns to its low-energy configuration. 5) Myosin head detaches and cycle repeats. Figure reproduced from [7] S. Garg et al, "Actomyosin filaments and ATP - heart of rigor mortis," *World Journal of Pharmaceutical Sciences*

2.1.2 Muscle Models of Force Production

There exist several models which allow for the approximation of net muscle force from physiological properties of the muscle. One of the first models, developed by Hill in 1938, approximates muscle tension as a function of shortening velocity, and establishes a force-length dependence. The model is the result of a second-order linear dynamic system, and can be represented by a network of springs, dampers, and masses. The resultant force relationship is represented as:

$$F = \frac{F_o\left(1 - \frac{v}{v_{max}}\right)}{1 - \frac{F_o}{a}\frac{v}{v_{max}}}$$

where F_o is the maximal tetanic force producible by all the myosin heads in the muscle's sarcomeres, a is a model constant, v is the net muscle contraction velocity, and v_{max} is the maximum possible muscle contraction velocity [8]. This relationship, while it is best representative for maximal tension contractions, is a good approximation for many different levels of activation and yields well-fitting results. However, a model which is derived more closely from the sliding filament model (ie, on the molecular level rather than on the myofibril level) will yield more thorough results.

A more recent theory by Descherevskii relates muscle force production to the number of active and inactive myosin heads, as described by the sliding filament theory. The Descherevskii kinetic model describes the muscle force as $F_s = f(n - m)$, where F_s is single sarcomere force, f is both the active and braking force of the myosin head, and n and m are the number of myosin heads in the force generation and detachment phases, respectively [9].

The development over time of both populations of contractile states, n and m, are expressed in first-order differential equations. The steady limit of these equations reduces to the Hill

relationship for force reproduced above. The unsteady limit of this kinetic theory is introduced in the following section, where it is incorporated into a dynamic model for lifting a weight. The Descherevskii theory is the critical relation which allows for the time integration of net muscle force from the molecular level of muscle contraction, and when integrated into a dynamic model allows for the derivation of large-scale joint trajectories.

2.2 Weightlifting

2.2.1 Kinematics of a Weightlift

In analyzing the kinematics and dynamics involved in a leg press, a simple two-joint model is used to derive the governing equations of motion. In this arrangement, the hip is free to translate relative to the foot along the ramp axis (z axis), and this motion is directly governed by the rotation angle about the knee. For the leg press machine utilized in these experiments, the chair is free to translate on an angled platform, which can be "loaded" with various weights. This dynamic system is represented in figure 4. The "ground" or "zero" position here is represented by the feet, and M_T, the mass of the torso and chair, is located at the hip. M_a, the mass of the

Table 1: Parameters used to describe kinematics of weighlift. Some average values are given, which were used in original model descriptions. For better accuracy, these values may be measured for individual athletes.

	Symbol	Unit	Estimate	Source
Limb length	L	m	Average male ~0.48m	[11]
Maximal possible lift mass	M^*	kg	Determined through testing	_
Mass of lower body limbs	M_a	kg	~20% of total mass	[11]
Mass of weights	M_w	kg	Varied in experiments	_
Mass of torso and chair	M_T	kg	~Remainder of total mass	_
Radius of joint	r	m	~.075*L	[12]
Cross-sectional area of muscle	A_{tot}	m^2	Approximated by leg measurements	_
Angle of ramp from horizontal	γ	radians	Varies with leg press machine (~π/6 at MIT Z Center)	_

lower body limbs, is concentrated at the knee, and the mass of the weights M_w translates with the same magnitude of velocity and acceleration as M_t. The parameters used to define the system are depicted in table 1.

The various masses and their ratios can be measured or estimated from anatomical data. The joint length L is measured, while the moment arm of the knee joint has been shown to range from 5-12 percent of limb length [12]. For analysis, a ratio r/L=7.5% is chosen.

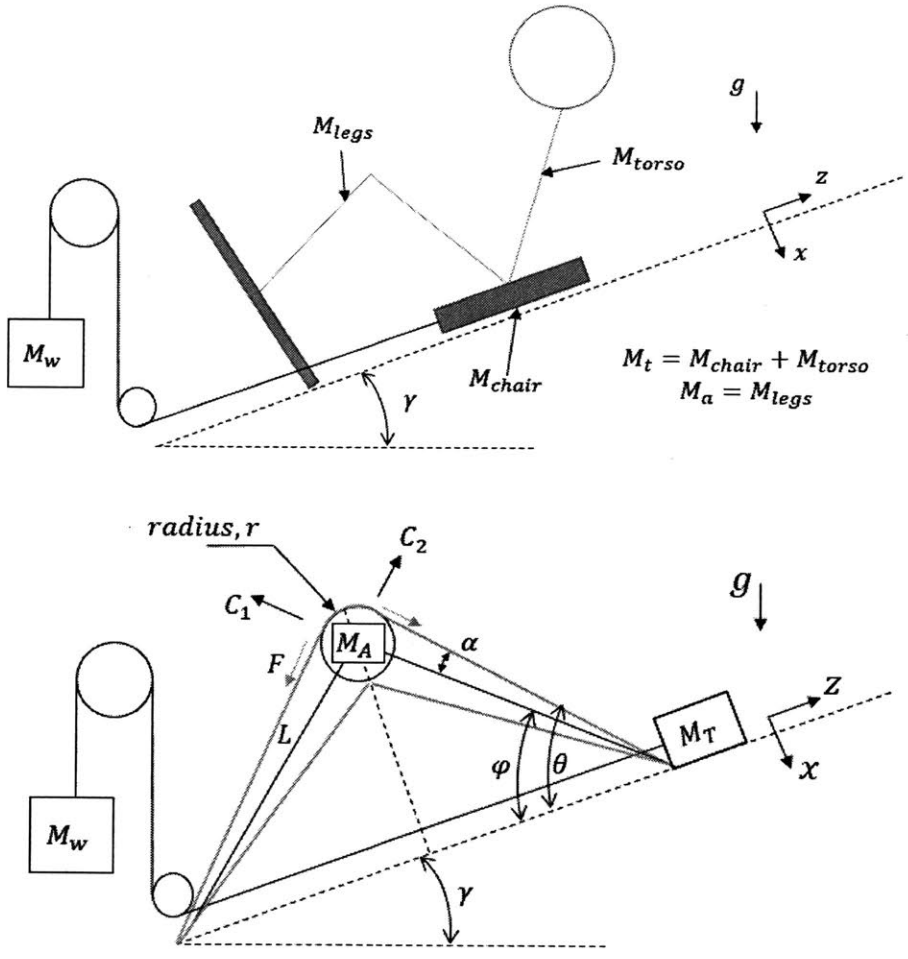

Figure 4: A dynamic model for lifting a weight, where muscle actuators supply a tension force F about a moment arm r, centered about a knee joint. The hip and foot are free to translate along a straight-line path in the z direction, determined by joint angle φ. The ramp is elevated from the horizontal at an angle γ to the horizontal.

The primary kinematic relationship of the system relates position of the mass $(0, z_M)$, position of the knee (x_k, z_k), and their derivatives with the angle of the joint to the vertical φ:

$$z_M = 2Lcos(\varphi)$$

$$\dot{z}_M = -2Lsin(\varphi)\dot{\varphi}$$

$$\ddot{z}_M = -2Lsin(\varphi)\ddot{\varphi} - 2Lcos(\varphi)\dot{\varphi}^2; \quad \ddot{z}_k = \frac{1}{2}\ddot{z}_M = -Lsin(\varphi)\ddot{\varphi} - Lcos(\varphi)\dot{\varphi}^2$$

$$\ddot{x}_k = -Lcos(\varphi)\ddot{\varphi} + Lsin(\varphi)\dot{\varphi}^2$$

The equation of motion about the knee, and about the hip, provide relations between the joint motion and interaction forces:

$$M_a\ddot{z}_k = (C_2 - C_1)cos(\varphi) - M_a g sin\gamma$$

$$C_1 cos\varphi = M_T(\ddot{z}_M + gsin\gamma) + M_W(\ddot{z}_M + g) + Fcos\theta$$

$$C_2 sin\varphi = -C_1 sin\varphi + 2Fsin\theta - M_a\ddot{x}_k + M_a g cos\gamma$$

The values for C_1 and C_2 have been derived as a function of joint angle φ and its derivates, as well as forces applied in the muscle F, via a force balance about the knee joint. Combining these three equations to eliminate C_1 and C_2, we obtain:

$$\left(1 + 4\left(\frac{M_T}{M_a} + \frac{M_w}{M_a}\right)\sin^2\varphi\right) * (\bar{\ddot{\varphi}}) + \left(4\left(\frac{M_T}{M_a} + \frac{M_w}{M_a}\right) sin\varphi\, cos\varphi\right) * (\bar{\dot{\varphi}})^2 =$$

$$\left(\left(1 + 2\frac{M_T}{M_a}\right) sin\gamma + 2\frac{M_W}{M_a}\right) sin\varphi - cos\gamma cos\varphi - \frac{2Fsin \propto}{M_a g}$$

Here, terms with overbars $(\bar{\dot{\varphi}}, \bar{\ddot{\varphi}})$ are non-dimensionalized derivative terms, the timescale T= $\sqrt{\frac{L}{g}}$ is used as the characteristic time parameter. This second-order nonlinear ODE, which relates φ to muscle contractile force F, provides the basis for an integration of the motion trajectories during a weightlift. The remainder of analysis of the model concerns the derivation of the force term F as a function of time and of various muscle parameters.

2.2.2 Non-linear Differential Equations for Muscle Trajectories: Single Fiber Type

Is has been shown that the most realistic numerical integration of this model is found when using the unsteady limit of Descherevskii's kinetic model to predict the muscle force [13]. Non-dimensionalizing the values n and m relative to the total number of myosin heads, α_D, the following relations result:

$$\frac{d\bar{n}}{dt} = \frac{1-\bar{m}-\bar{n}}{\bar{\tau}_1} - \frac{\tilde{v}\bar{n}}{\bar{\tau}_2}$$

$$\frac{d\bar{m}}{dt} = \frac{\tilde{v}\bar{n}}{\bar{\tau}_2} - \frac{\bar{m}}{\bar{\tau}_2}$$

$$\tilde{v} = v/v_{max} = -G(\bar{\varphi}) \quad [9]$$

Here, both $\bar{n}$ and $\bar{m}$ are non-dimensionalized parameters of the values n and m, scaled by the total number of myosin heads in half a sarcomere, α_D. Therefore, $\bar{n}= n/\alpha_D$, and $\bar{m}= m/\alpha_D$. Both $\bar{n}$ and $\bar{m}$ are functions of a variable $\tilde{v}$, which is a ratio of the muscle contraction velocity to its maximum contraction velocity, and can be written as a function of $\bar{\varphi}$, which scales with the model parameter G. G here represents a geometric relationship between muscle contraction velocity and angular velocity of the joints. Here, the non-dimensional timescales τ_1 and τ_2 are introduced; τ_1 represents the characteristic time of transition of a myosin head from attachment to force generation states, while τ_2 is the characteristic time of transition from detachment to attachment phases. Both parameters are non-dimensionalized, notated by overbars: $\bar{\tau}_1 = \tau_1\sqrt{g/L}$, and $\bar{\tau}_2 = \tau_2\sqrt{g/L}$. For the purposes of a single uniform fiber-type muscle model, the variables G and $\bar{\tau}_2$ are model fit parameters, which remain constant. However, in the introduction of a fiber-type-dependent model, these parameters are quite dynamic and highly dependent upon muscle fiber composition. The non-dimensional force is directly proportional to

the difference in $\bar{n}$ and $\bar{m}$, and absolute force scales as a proportion of the maximal force the muscle can produce.

$$\bar{F} = \bar{n} - \bar{m}, \text{ where } \bar{F} = \frac{F}{F_o}$$

The term F_o represents the maximum producible muscle force, which is related linearly to the maximal mass the person can lift by the following expression:

$$\frac{F_o}{g}\left(\frac{r}{L}\right) - \left(M_T + \frac{M_a}{2}\right) sin\gamma = M^*$$

Rearranging, F_o can be expressed by:

$$F_o = gM_a \frac{L}{r}\left(\frac{M^*}{M_a} + \left(\frac{M}{M_a} + \frac{1}{2}\right) sin\gamma\right)$$

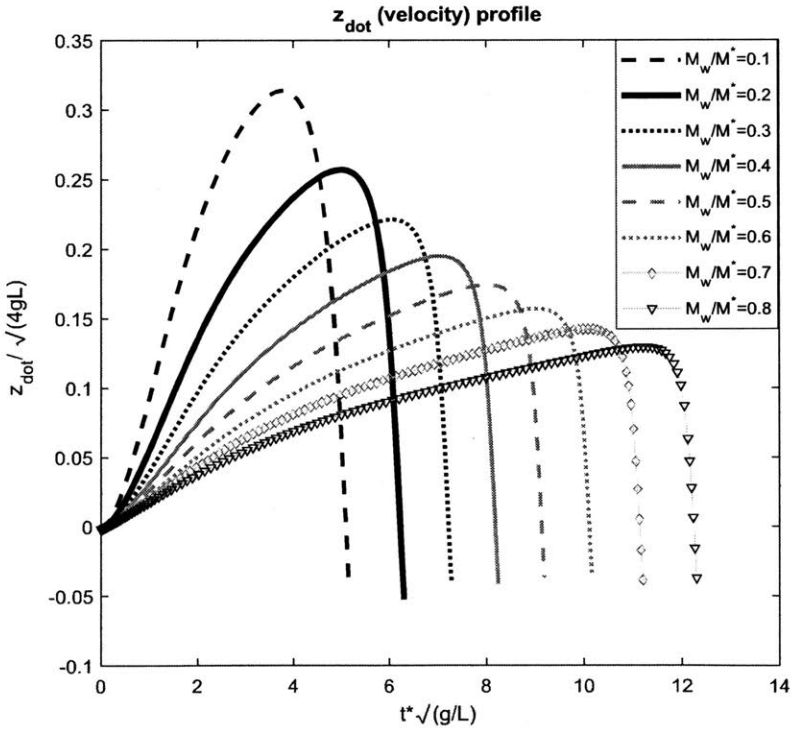

Figure 5: The output velocity trajectories of the dynamic weighlifting model, using Descherevskii kinetic force theory for the force input. All input parameters were held constant, while the value M_w/M^* was varied (the ratio of the weight lifted to the maximal possible weight).

These equations then define all necessary variables to integrate this coupled set of ODEs forward in time to obtain a weightlift trajectory. Initially, the model is integrated by holding all variables constant and varying the ratio of mass lifted to maximum possible mass, M_W/ M^*. Numerically integrating the system of differential equations forward in time, with a state space representation of the variables φ, F, r and m, and their derivatives, the trajectories depicted in figure 5 & 6 result. The chosen input parameters to the model were: $\bar{\tau}_2 = .04$ and $\bar{\tau}_1 = 6\bar{\tau}_2$, G=0.17, and $\frac{M^*}{M_a} = 15$. The initial conditions were defined such that the knee starts in a completely bent position, $\varphi(0) = \frac{\pi}{2}$, and with zero initial velocity $\dot{\varphi}(0) = 0$.

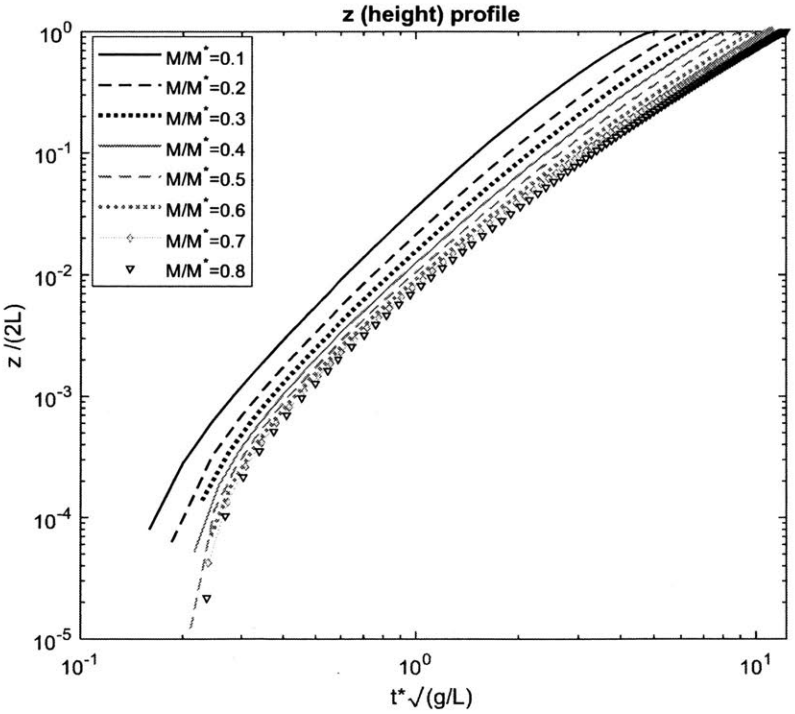

Figure 6: The output position trajectories of the dynamic weighlifting model, plotted on log scale axes, varying the value of M_w/M^*. The results asymptotically approach a slope of 2, or a quadratic relationship of position vs. time (position and time axes were scaled to be non-dimensional numbers).

For smaller masses lifted, the curves reach peak velocity earlier and have higher absolute peak velocities than at larger masses. When lifting weights close to the person's maximal possible

mass, the velocity curves "flatten" and elongate, and this trend is reflected in experimental data (the bigger the weight, the longer it will take to lift it and the slower the lift will be).

The trends revealed in the velocity trajectories here not only suggest the effectiveness of this analytical weightlifting model, but also open up doors for its potential use in medical applications or sports science. While this simplified model assumes uniform fiber type and contraction velocity, it can be extrapolated to include various fiber type populations, which is the process explored in this study through dynamic analysis and experimental methods. In muscle force production, fibers contract sequentially—ie, slow twitch fibers contract until more force is needed, after which fast-twitch fibers are "added in" as needed to produce the desired force. Therefore, for values of $\frac{M_w}{M^*}$ close to one, nearly all fibers must be recruited to complete the lift. Furthermore, it was speculated that by fitting experimental lift data to model curves in this regime, the necessary model parameters could be "back calculated," such as net contraction velocity and peak force production. In other words, we aim to use the velocity trajectories measured during a weightlift to estimate an athlete's fiber type makeup using fit parameters, which are characteristic to different muscle fiber types. These analytic methods are explored in the following section.

3. Methods: A Dynamic Muscular Model with Two Fiber Types

Two distinct fiber populations are introduced into the model developed above, by utilizing known and estimated properties, which distinguish the different types of muscle fibers. The main distinguishing features between Type I and II fibers are their contraction velocities and forces. While the contraction velocities are significantly higher in fast-twitch fibers, many studies have failed to prove that fast twitch fibers produce any more force than slow-twitch ones. The general

approach used was to treat the muscle as a "net" of contractile elements with an effective velocity v and force F, which are functions of the ratios and distribution of the fibers inside. The methods used to create these functions are developed using a simple fiber "matrix" dynamic model.

3.1 Impact of Fiber Type on Model Parameters

The model parameters that have yet to be defined more clearly are G and $\bar{\tau}_2$, in that in the uniform fiber model they are estimated using overall muscle characteristics. Their defining equations depend primarily on the maximum possible contraction velocity of the muscle, v_{max} (this was approximated as 1 meter/second in the uniform fiber model). G, which is a constant mapping contraction velocity to joint angular velocity, scales as:

$$G = \frac{r}{v_{max}}\sqrt{\frac{g}{L}}$$

$\bar{\tau}_2$ is a non-dimensional timescale, or a characteristic time for a single sliding filament contraction. This can be approximated by the following:

$$\bar{\tau}_2 = \tau_2\sqrt{\frac{g}{L}} = \frac{N_{sc}l}{v_{max}}\sqrt{\frac{g}{L}}$$

where N_{sc} is the number of sarcomeres aligned in series in a muscle, and l is the length of a single sarcomere "power stroke," or the sliding translational distance between an actin and myosin filament in a single contraction [13]. Determining the value of τ_2 also indirectly computes the value of τ_1, a secondary timescale utilized by the model. From relations developed by Wilkie [14], it is known that $\tau_1 \approx 4\tau_2$.

Both τ_2 and G are inversely proportional to the value of v_{max}, which is a function of muscle properties, primarily muscle fiber type and distribution. The contraction velocities of various fiber types is well-documented, so it is possible for v_{max} to be extrapolated from individual fiber

Table 2: Fiber "Matrix" Model Parameters							
Properties of Singular Muscle Fibers							
Parameter	Slow-Twitch			Fast-twitch			Source
	Symbol	Value		Symbol	Value		
Maximum force	F_s	$.57 \pm .08 \times 10^{-3}$	N	F_f	$.71 \pm .09 \times 10^{-3}$	N	[16]
Length	L_s	$2.09 \pm .01 \times 10^{-3}$	m	L_f	$2.09 \pm .01 \times 10^{-3}$	m	[16]
Fiber Diameter	D_s	$100 \pm 8 \times 10^{-6}$	m	D_f	$101 \pm 8 \times 10^{-6}$	m	[16]
Cross-sectional area	A_s	7.85×10^{-9}	m^2	A_f	8.01×10^{-9}	m^2	—
Number aligned in series in muscle	N_s	$= L/L_s \approx 150$	[ ]	N_f	$= L/L_f \approx 150$	[ ]	—
Mechanical Stiffness	k_s	(Unknown)	N/m	k_f	(Unknown)	N/m	—
Contraction Velocity (fiber lengths/sec)	v_s	$1.66 \pm .20$	F.l./s	v_f	$3.42 \pm .43$	F.l./s	[17]
Sliding velocity	$v_{s,s}$	$= v_s L_s$	m/s	$v_{s,f}$	$= v_f L_f$	m/s	—
*Properties of Singular Sarcomeres**							
Parameter	Slow-Twitch			Fast-twitch			Source
	Symbol	Value	Unit	Symbol	Value	Unit	
"power stroke"	l	$11 \pm 2.6 \times 10^{-9}$	m	*			[18]
Length	l_{sc}	2.5×10^{-6}	m				[13]
Cross-sectional area	a	2.5×10^{-13}	m^2				[13]

Number aligned in series in muscle	N_{sc}	$= L/l_{sc}$ $\approx 10^5$	[]				—
*For the purposes of this model, the dimensional properties of sarcomeres are assumed to remain the same between various motor units.							

contraction velocity, if the fiber ratio is known. The various dimensional and dynamic parameters, characteristics of both muscle fibers and sarcomeres, are displayed in Table 2.

3.2 Prediction of Net Contraction Characteristics

The development of fiber "matrix" models allows for the mapping of muscle fiber properties to muscle properties as whole, as it is assumed that the fibers are arranged in a grid-like pattern in the muscle. In this assumption, the fiber velocities add along the direction of contraction, and forces add cross-sectionally (perpendicular to the direction of contraction).

While the exact arrangement of slow-twitch versus fast-twitch fibers is unknown, it has been shown to vary between muscle groups in the body. For example, the inferior pharyngeal constrictor in humans has been found to have a slow inner layer with primarily Type I fibers, and a fast outer layer containing primarily Type II [15]. However, in the majority of skeletal muscle the arrangement can be approximated as relatively randomly distributed fiber type. In the following sections, we explore the implications of various striation patterns on the relationship between the individual fiber velocities and net muscle velocities.

For the purposes of this analysis, the fibers are arranged in a grid and connected into long fiber strands by weak springs, which allow for varying velocities between strands. One end of the muscle is "fixed," while the other end connects all the fibers via a rigid, massless "plate" which is free to translate along the direction of contraction. First analyzing a case in which bands of

fibers are aligned horizontally (see figure 7), or perpendicular to the direction of contraction, the contraction velocities add linearly. In this case, all strands have identical velocities, so the springs play no role in storing elastic energy.

Using the parameters defined in table 2, the net velocity is then expressed in a simple relation as:

$$v_{max} = (1 - R)N_s v_{s,s} + RN_f v_{s,f}$$

where R is the critical value this study aims to quantify: the ratio of the number of fast twitch fibers to total number of fibers. A value of R=0 indicates the athlete has only slow twitch fibers in a particular muscle, and R=1 indicates there are only fast twitch fibers. All muscles will lie on a fraction between these two extremes, and as we see here, the net velocity is a weighted sum of

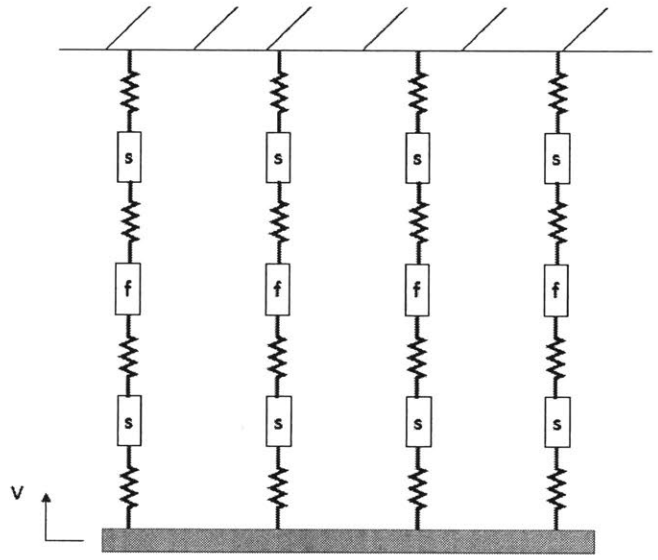

Figure 7: A Horizontal striation matrix model. Similar types of fibers are arranged into bands which are perpendicular to the direction of the velocity.

the two velocities, scaled by the ratio R. The above equation can be simplified further if the sliding velocities are expressed in units of fiber lengths per second:

$$v_{max} = (1 - R)v_s L_s \left(\frac{L}{L_s}\right) + Rv_f L_f \left(\frac{L}{L_f}\right) = (1 - R)v_s L + Rv_f L$$

This relation, while it directly represents the horizontally striated case, is also a very good approximation for a randomly-distributed arrangement. In a random arrangement, if the percentage of fibers in each strand is roughly the same as the percentage in the whole muscle, then each strand will have a net velocity equal to the v_{max} derived above.

If instead a vertically striated arrangement is analyzed (which has been shown to exist in some areas of human muscle) the analysis becomes slightly more complicated. In this arrangement, each strand will pull with a different velocity, leading to an elastic energy storage in the muscle strands. This arrangement is modeled as a system of weak springs connecting the fibers in each strand, and a virtual work analysis yields an expression for the forces felt by the springs over an infinitesimal time, Δt. Therefore, the deformation in a single fast-twitch fiber, and furthermore the force felt in the strand, may be expressed as a function of the difference between the net contraction velocity and the total contraction velocity of the fiber:

$$\Delta x_f = (v - v_{s,f}N_f)\Delta t$$

$$F_f = k_f * \Delta x_f = k_f(v - v_{s,f}N_f)\Delta t$$

where Δx_f and $v_{s,f}$ are the displacement and velocity of the fast twitch strand, respectively. An identical relationship holds for the slow twitch strands, instead with slow-twitch fiber properties:

$$F_s = k_s * \Delta x_s = k_s(v - v_{s,s}N_s)\Delta t$$

Using this expression for the force felt in the end "plate" of the muscle, due to an individual fiber strand, the expression for net strain felt at the plate is:

$$\sigma_{tot} = \frac{k_f \varphi_f \Delta t}{A_f}\left(v - v_{s,f}N_f\right) + \frac{k_s \varphi_s \Delta t}{A_s}\left(v - v_{s,s}N_s\right)$$

Where φ_f and φ_s are the number of fast-twitch and slow-twitch strands in the muscle, respectively, and k and A are the respective stiffnesses and cross-sectional areas of the fibers. It

is then assumed that the muscle contraction velocity is "chosen" by the central nervous system such to minimize the net strain felt by the muscle. At minimum strain values, the following relation results for net velocity v as a function of φ_f and φ_s:

$$v = \frac{\frac{k_f \varphi_f}{A_f}(v_{s,f} N_f) + \frac{k_s \varphi_s}{A_s}(v_{s,s} N_s)}{\frac{k_f \varphi_f}{A_f} + \frac{k_s \varphi_s}{A_s}}$$

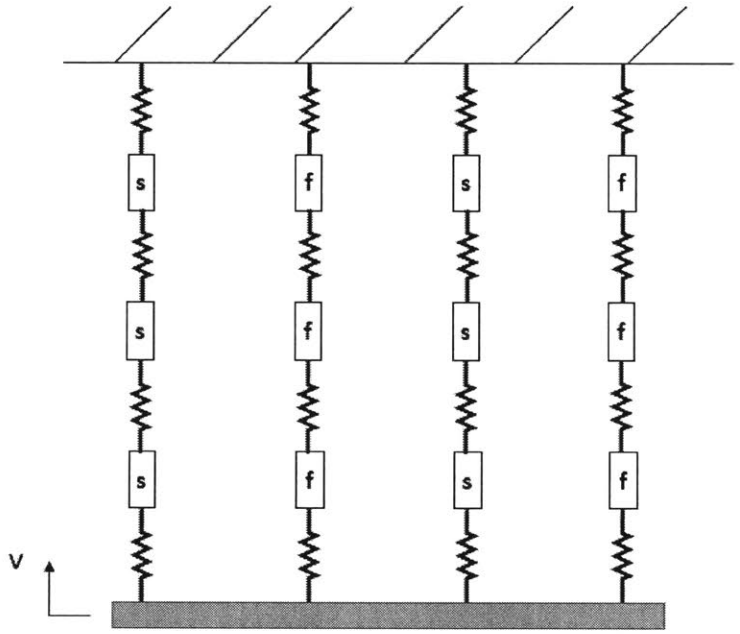

Figure 8: A Horizontal striation matrix model. Similar types of fibers are arranged into bands which are parallel to the velocity of contraction.

To express the relation derived above as a function of the ratio R, geometric relations provide a relationship between φ_f and φ_s, and R:

$$\mathrm{R} = \frac{total\ fast\ fibers}{total\ fibers} = \frac{\varphi_f N_f}{(\varphi_s N_s + \varphi_f N_f)}$$

By cross-sectional area constraints, the following area constraint is known:

$$A_{tot} = A_s \varphi_s + A_f \varphi_f$$

Rearranging, it results:

$$\varphi_f = \frac{A_{tot}}{\left(\frac{N_f}{N_s}\right)\left(\frac{1}{R} - 1\right)A_s + A_f}$$

$$\varphi_s = \frac{\mathrm{A_{tot}}}{\mathrm{A_s}} - \frac{A_f A_{tot}}{\left(\frac{N_f}{N_s}\right)\left(\frac{1}{R} - 1\right)A_s^2 + A_f A_s}$$

These expressions can be substituted into the equation for $v = f(\varphi_f, \varphi_s)$ to obtain a full relation between v and R in the vertically striated arrangement:

$$v = \frac{\frac{N_s}{N_f}\frac{A_s}{A_f}\left(\frac{k_f}{k_s}\right)\left(\frac{R}{1-R}\right)v_{s,f}N_f + v_{s,s}N_s}{\frac{N_s}{N_f}\frac{A_s}{A_f}\left(\frac{k_f}{k_s}\right)\left(\frac{R}{1-R}\right) + 1}$$

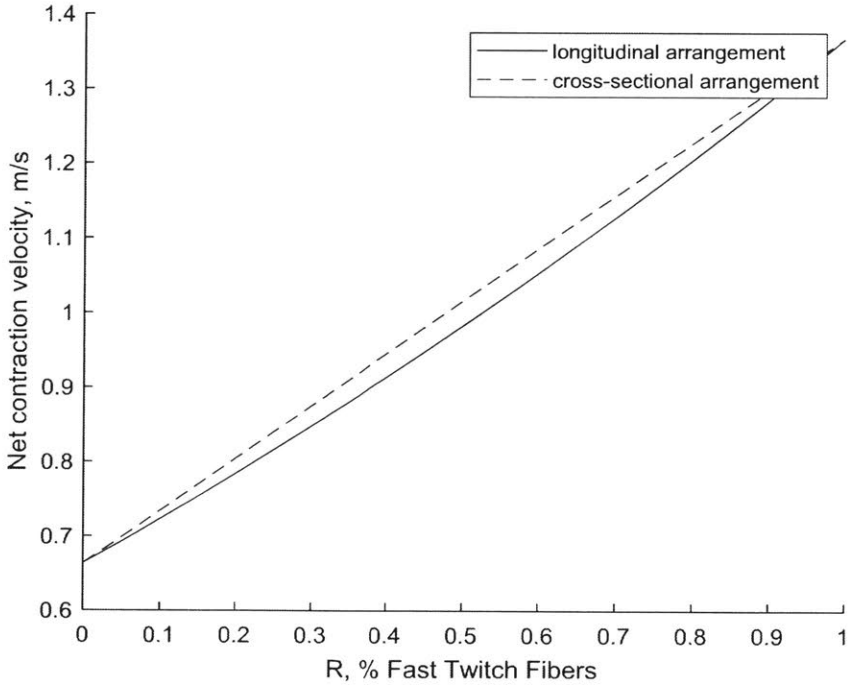

Figure 9: Relationship between net muscle contraction velocity as a function of % fast twitch fibers. A linear relationship results from a cross-sectional striation pattern, and a longitudinal striation pattern results in a slight deviation in the linear relationship. In most human skeletal muscle, it is postulated that the fibers are nearly randomly dispersed, which would result in a relationship which lies between these two curves. Using biologically relevant parameters, the maximum difference between the velocities is ~5%.

Comparing the vertically striated arrangement to the horizontal arrangement and applying appropriate boundary conditions for $v_{s,s}$ and $v_{s,f}$, the curves for *v=f (R)* begin and end at the

same values (the all-slow or all-fast twitch cases), but deviate for intermediate values (depicted in figure 9). The curvature of the vertically striated relationship is highly dependent on the ratios between cross-sectional areas and dynamic stiffnesses of the fibers. Here, it is assumed the stiffnesses are identical, but that fast-twitch fibers are slightly larger, which is supported by the literature (see table 2 for parameter values utilized).

3.3 Predicted Muscle Trajectories with Dependence on Fiber Ratio

With all of the necessary model parameters defined, it is possible to numerically integrate the dynamic equation for joint angles in time, as previously introduced. However, we now aim to analyze the model as a function of fiber type; the variable which changes with fiber type ratio R is v_{max} (net muscle contractile velocity), which is incorporated into the Descherevskii kinetic

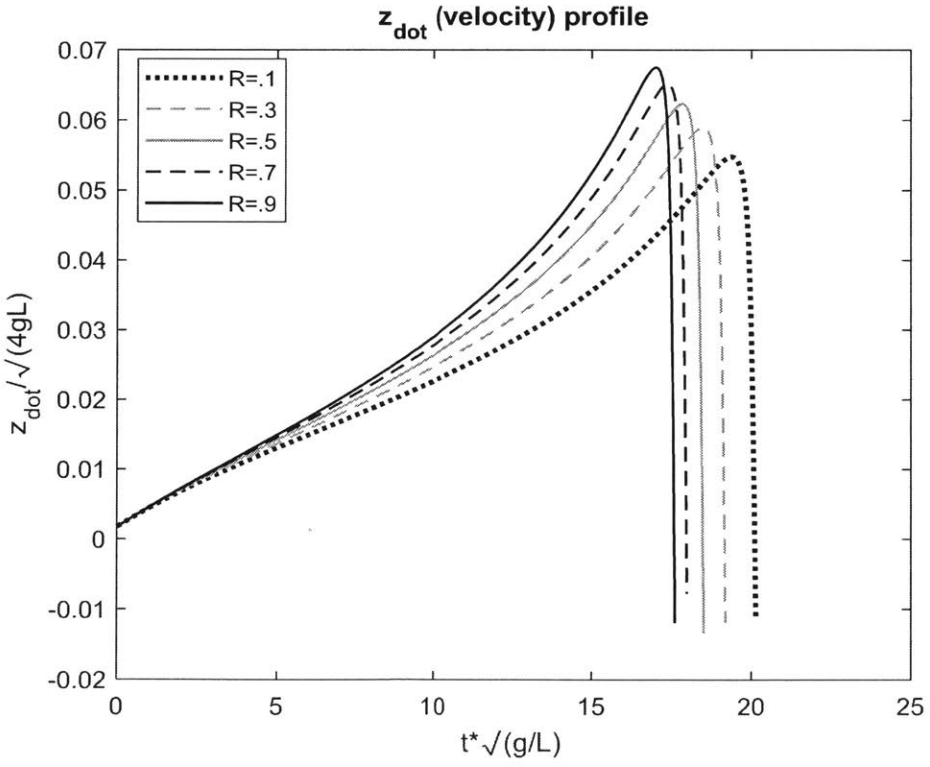

Figure 10: Joint velocity trajectories over time for various values of R (% fast twitch fibers). Model parameters were fixed at: M_W/M^*=0.99, M^*/M_a=10, M_T/M_a=5, and r/L= 0.075.

model for net force. As a result, the joint trajectories for velocity over time are now varied with fiber type ratio R, as shown in figure 10.

As expected, the model predicts shorter times to peak and larger peak velocities for athletes with higher ratios of fast-twitch fibers, with all other model parameters held constant. Conversely, more slow-twitch athletes take longer to complete the lift, and see lower peak velocities.

In order to further study the effects of fiber type ratio on predicted results, the time to peak as a function of percent of max weight is plotted for various values of R (shown in figure 11). While the slopes of each of the curves remain relatively similar for all values of R for a fixed value of M_w/M^*, the times to peak are consistently higher for lower values of R. This is an intuitive result, in that athletes with slower twitch muscle compositions will take longer to complete the lift than more fast-twitch athletes, independent of the mass being lifted.

As M_w approaches M^*, the time to peak velocity as predicted by the model approaches infinity. For this reason, the model is not a completely realistic representation of a lift. While athletes in experiments may lift at maximal exertion, a lift will be completed in finite time. It is possible then that experimental results at maximal exertion operate in lower regimes of M_w/M^* in the model. In the next section, experimental data are compared to these model-derived results, in order to analyze the validity of such a model for fiber type estimation.

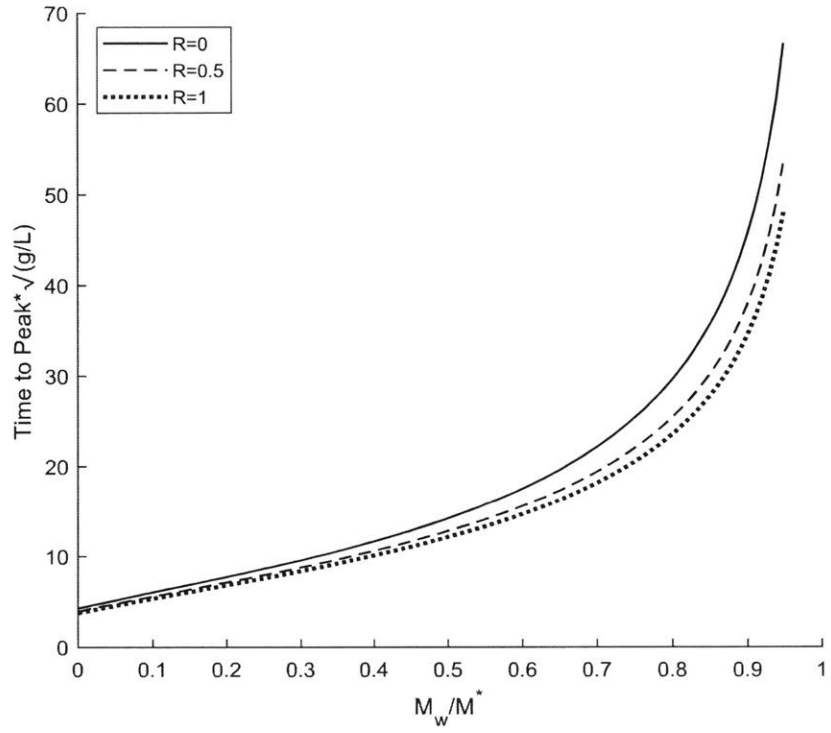

Figure 11: Non-dimensional Time to Peak vs. M_w/M^*. Most notably, the time to peak approaches infinity as the athlete attempts to lift their maximal mass. The times to peak are consistently larger for smaller values of R. Critical model parameters chosen were: $\frac{r}{L} = 0.075$, $0 < \frac{M_w}{M_a} < 6$, $\frac{M^*}{M_a} = 10$, $\frac{M_T}{M_a} = 1$.

4. Methods: Experimental Validation

In order to analyze the potential of this work as a tool to measure athlete muscle composition, experimental data was gathered from members of the MIT Cycling Team. A weightlifting test was performed, in which each subject lifted their maximum weight on a leg press machine. The machine was a leg press such that the legs extend as the weight is pushed, and the chair slides outwards away from the footboard (see experimental setup, figure 12). The weight lifted was

varied by changing the masses attached to the cables by moving a small indicator rod. Each athlete started the lift at an inner leg angle (at the knee) of approximately 70 degrees.

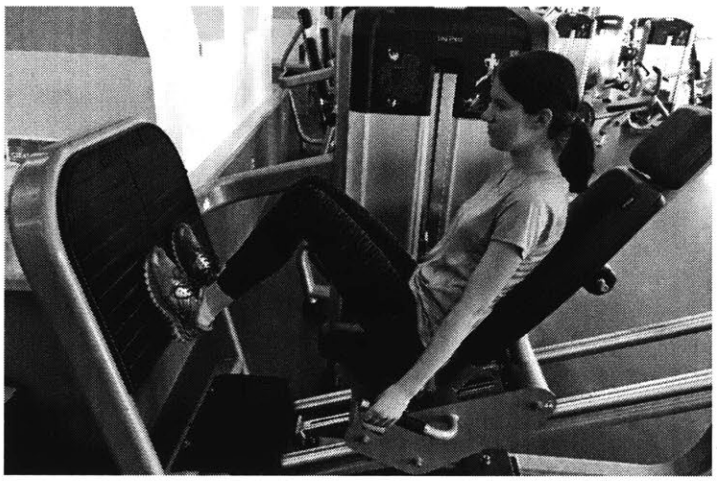

Figure 12: Experimental Setup on a leg press machine in the MIT Z Center. In this machine setup, the footplate was stationary, and chair was free to translate along an elevated ramp. An IPhone with accelerometer was placed on the moving weights inside the machine, and all athletes started the lifts from an initial inner leg angle of ~70 degrees.

Output accelerations of the weights (and therefore, accelerations of the chair) were recorded using the Engineering Toolbox IPhone App, at a sampling rate of 100 Hz. The acceleration data was integrated in time, and offsets were subtracted from the data to account for accelerometer "drift." The start and end of the lift were manually identified in each of the data sets: the start was identified as the onset of a significant time period held above zero velocity, and the end of the lift as the onset of negative velocity. Resultant velocity profiles for the lift were compiled and compared between athletes (see figure 13).

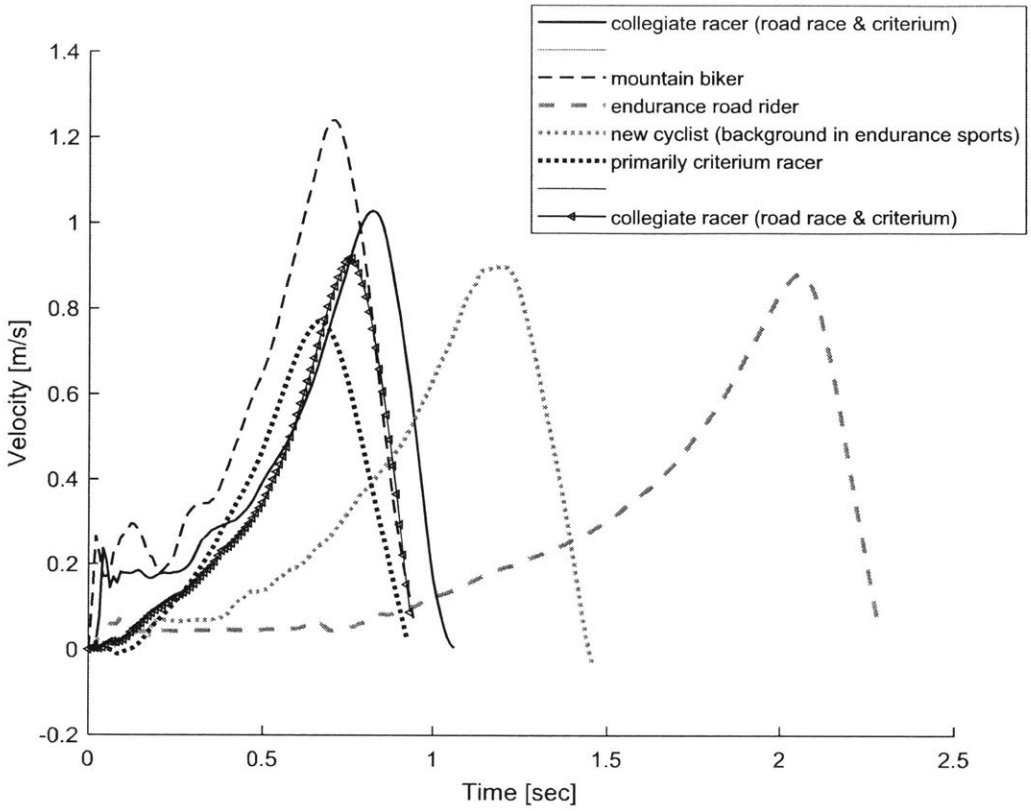

Figure 13: The velocity trajectories obtained by integrating accelerometer data from a single leg press for various competitive cyclists. The data shows a broad range of timescales for the lift, suggesting both different strength characteristics and muscle composition between athletes.

As shown in figure 13, the experimental data demonstrates vastly varying lift profiles, with times to peak ranging from little over 0.5 seconds to longer than two seconds. These widely varying results suggest the athletes sampled had different strength values (M*), as well as varying muscle twitch compositions. While all of the athletes were cyclists, their backgrounds within the sport were quite different, which affected their training, and as a result, likely their muscle composition. The curve with highest peak belonged to an experienced mountain biker, the other three black curves were data from experienced road bike racers (both criterium and road race), the gray dotted curve represents a road cyclist competing primarily in endurance events, and the gray dashed curve represents an athlete relatively new to the sport of cycling,

with a background in other endurance sports. These results suggest that both mountain biking and criterium racing train more fast-twitch fibers, or involve more short-duration, explosive efforts. In competitive cycling, criteriums are often dominated by good sprinters, which appears to confirm the idea that these athletes might have higher ratios of fast twitch fibers.

These ideas are further explored by comparing the model predictions for peak velocity and time to peak for various fiber type ratios. For the cycling data, three lifts were performed for each athlete, and the mean and standard deviation are calculated and plotted relative to model-predicted curves (see figures 14 and 15).

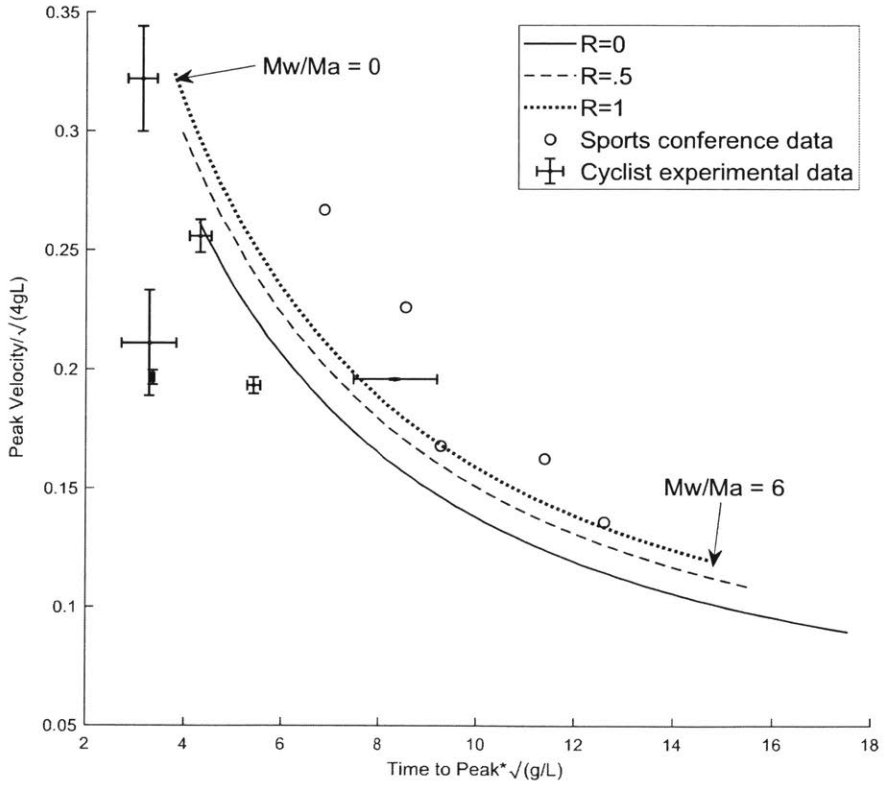

Figure 14: Non-dimensional Peak Velocity vs. Time to Peak, comparing model-predicted curves to experimental data points. Points with errorbars represent data collected from the MIT Cycling Team, and circles represent data collected from a prior conference. The cyclist datapoints are a mean over three trials, and errorbars indicate standard deviation. For each R curve, the variable $\frac{M_w}{M_a}$ was varied. Critical model parameters chosen were: $\frac{r}{L} = 0.075$, $0 < \frac{M_w}{M_a} < 6$, $\frac{M^*}{M_a} = 10$, $\frac{M_T}{M_a} = 1$.

The three model curves plotted demonstrate that the mass lifted, in relationship to their limb mass, has a considerably greater impact on the resultant peak velocity and time of their lift than their fiber ratio R. From $0 < \frac{M_w}{M_a} < 6$, the resultant curve for a single value of R spans an order of magnitude of variation in time to peak. Increasing R results in shifting this predicted curve upwards in velocity and decreased time. If instead $\frac{M_w}{M_a}$ is fixed at different values and R is varied from 0 to 1, the resulting curves are shown in figure 15.

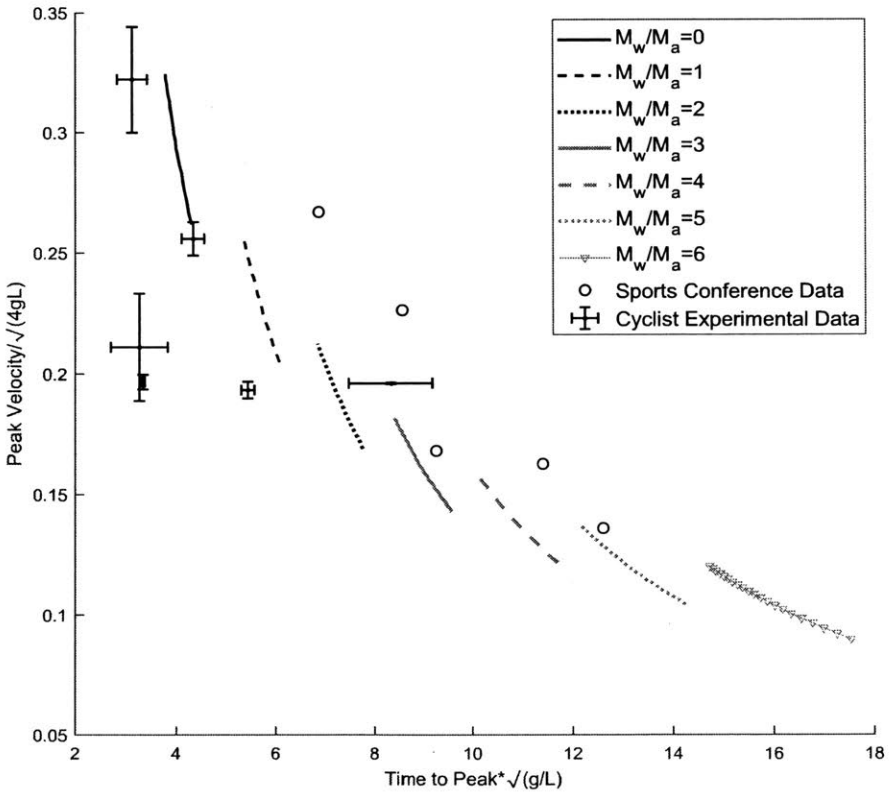

Figure 15: Non-dimensional Peak Velocity vs. Time to Peak, comparing model-predicted curves to experimental data points. Points with errorbars represent data collected from the MIT Cycling Team, and circles represent data collected from a prior conference. The curves represent model-predicted values: for each curve, the variable $\frac{M_w}{M_a}$ was held constant and R (% fast twitch fibers) was varied from 0 to 1. R=1 represents the top (peak velocity) of each curve, and R=0 is the lower end of each curve. Critical model parameters chosen were: $\frac{r}{L} = 0.075$, $0 < \frac{M_w}{M_a} < 6$, $\frac{M^*}{M_a} = 10$, $\frac{M_T}{M_a} = 1$.

In figure 15, the various values of $\frac{M_w}{M_a}$, under identical model constraints to figure 14, outline the same set of curves. However, varying R results in generally steeper, shorter curves than by varying $\frac{M_w}{M_a}$. Between R=1 (the upper end of each curve) and R=0 (the lower end), the change in non-dimensional peak velocity predicted is ~0.05, and variation in time to peak ranges from near zero for low weights and ~2 for large $\frac{M_w}{M_a}$. The model predictions then suggest the peak velocity and time to peak we observe are functions of all of these parameters $(\frac{M_w}{M_a}, \frac{r}{L}, R)$, which vary significantly from athlete to athlete, and between various lifts. While the effect of moment arm ratio $\frac{r}{L}$ on results has not yet been explored in detail, this ratio is thought to remain relatively constant between individuals, despite variations in limb length.

It is notable that nearly all experimental datapoints lie on or close to the model-predicted regime $0 < \frac{M_w}{M_a} < 6$, or $0 < \frac{M_w}{M^*} < 0.6$. While the experiments were performed at or very close to each of the athletes' maximal effort, they correspond only up to 60 percent exertion in the model-predicted trajectories. This primary disconnect between the model and experimental data may be attributed to the mathematical nature of a muscle model: physical laws suggest max or near-max efforts may take near-infinite amounts of time, but this is not predictive of real muscle activity. Explosive efforts are completed in a finite, usually relatively short, period of time, meaning that real data may match more closely with "easier" efforts as predicted by the model. However, the mapping of time to peak versus $\frac{M_w}{M^*}$ for experimental data, similar to the model data shown in figure 11, may reveal new trends not visible in the data gathered only at M^*.

5. Discussion

In analyzing the relationship between experimental datapoints and model-predicted curves, both data sets lie within or near to the bounds set by the model predictions. With further refinement of the experimental process and experimental testing on more types of athletes, it is possible that the data could converge to a more definitive pattern. However, with the current data, an apparent trend is visible which predicts lower peak velocities with increased time to peak, which according to the model, corresponds with a larger ratio of slow twitch fibers. Conversely, the trends show higher peak velocities with shorter lift times, corresponding to more fast twitch fibers.

These trends suggest the potential for this method to be used as both a muscle "diagnostic" tool and a training tool. The one-rep max velocity profile could indicate where an athlete falls on a spectrum (of R, muscle composition) relative to other athletes, and relative to model-predicted curves. This might inform an athlete of their muscle fiber pre-disposition, allowing them to know which types of sports they might be well-suited for, or indicating areas for improvement in their current sport. Additionally, with one-rep max press tests interspersed throughout the course of a training plan, the velocity output data might be used to track progress towards an athletes' specific training goals. Collecting lift data for various levels of exertion, M_w/M_a, allows for the creation of curves similar to those calculated in figure 11. An apparent shifting of the curves (either shorter/longer time to peak or greater/lesser peak velocity) would indicate either a trend in athlete strength or in muscle fiber composition. Both potential applications, in "diagnostic" and in progressive "tracking" applications, have immediate potential in training for professional and amateur athletes alike.

Further refinements to the experimental process might allow for a closer fitting to model-predicted data. Such improvements might include the use of a higher-precision accelerometer or

velocity measurement system for obtaining velocity trajectories. In the experimental protocol itself, a method for maintaining a fixed initial knee angle between trials would be extremely beneficial. Because of the difficulties of accurately measuring joint angles in real-time, starting angles for each of the lifts were near the nominal value (70 degrees), but not entirely consistent from one subject to another. A method for improving the accuracy of this initial angle would likely improve the overall precision of the test results, allowing for more reliable comparisons between tests on different machines, and between different athletes.

Other experimental variables that should be considered in future testing are the frictional components of the leg press machines, and the type of machine. It was assumed in my analysis that all machines operated with zero friction, which may not be a sound approximation for all leg press machines. Similarly, my experimental trials were all performed in an upright leg press; however, it is very common for leg presses to be "inverted," in which the athlete sits in a chair with the back facing the ground and pushes nearly vertically upwards on the weights. While the dynamics of the lift are similar between types of machines, tests on both types of machines might yield varying results. Further work on this testing method will likely focus on standardizing the test protocol between various machines, and improving consistency in results between machines and various test environments.

6. Conclusions

This study demonstrates the potential for a single weightlift test near maximum effort to be a powerful tool for analyzing athlete muscle characteristics—particularly, fast vs. slow twitch muscle fiber composition. The development of a dynamic muscle model, which includes two populations of fibers, allows for the prediction of resulting curves from basic athlete physiological data and muscle properties. Similarly, the model in combination with experimental data allows for the prediction of muscle properties from joint velocity profiles. The current strengths of the model lie in its ability to "map" athletes relative to one another, and to allow athletes to track training progress over time, with the knowledge of their peak velocity and peak time for leg press tests. Additionally, this type of analysis introduces a dynamic relationship between muscle fiber contractile properties on the micro-scale and whole muscle contractile properties, considering several fiber type populations. The analysis proves to be not only interesting from a biological physics and dynamical modeling perspective, but also carries immense potential in sports science and training applications.

References

[1] J. R. Karp, "Muscle Fiber Types and Training," *Strength and Conditioning Journal*, vol. 23, no. 5, p. 21, 2001.

[2] K. Punkt, *Fibre types in skeletal muscles*. Berlin: Springer, 2002.

[3] "Physiology of the Muscular System," *Basicmedical Key*, 25-May-2016. [Online]. Available: https://basicmedicalkey.com/physiology-of-the-muscular-system/. [Accessed: 27-Apr-2018].

[4] N. Hogan, "Muscle Physiology," *Biomechanics & Neural Control of Movement, Course Notes*, Sep. 2017.

[5] E. Sierra, A. Fernández, A. E. D. L. Monteros, M. Arbelo, Y. B. D. Quirós, and P. Herráez, "Muscular senescence in cetaceans: adaptation towards a slow muscle fibre phenotype," *Scientific Reports*, vol. 3, no. 1, Jul. 2013.

[6] E. R. Kandel and S. Mack, *Principles of neural science*. NY, NY: McGraw-Hill Medical, 2014.

[7] S. Garg, S. Mittal, and N. Gupta, "Actomyosin filaments and ATP - heart of rigor mortis," *World Journal of Pharmaceutical Sciences*, vol. 4, no. 9, pp. 398–402, Aug. 2016.

[8] A. V. Hill, "The Heat of Shortening and the Dynamic Constants of Muscle," *Proceedings of the Royal Society B: Biological Sciences*, vol. 126, no. 843, pp. 136–195, Oct. 1938.

[9] V. Deshcherevskiĭ, "A kinetic theory of striated muscle contraction," *Biorheology*, vol. 7, no. 3, pp. 147–170, Jan. 1971.

[11] S. Plagenhoef, F. Gaynor Evans & T. Abdelnour "Anatomical Data for Analyzing Human Motion," *Research Quarterly for Exercise and Sport*, 54:2, 169-178, 2013. DOI: 10.1080/02701367.1983.10605290

[12] Visser, J.J., Hoogkamer, J.E., Bobbert, M.F. et al. "Length and moment arm of human leg muscles as a function of knee and hip-joint angles." *Journal of Applied Physiology.* 61: 453, 1990. https://doi.org/10.1007/BF00236067

[13] C. Cohen, BD. Texier, G. Laffaye, L. Auvray, C. Clanet "Weightlifting and the actomyosin cycle." *Proc. Royal Society A* 471: 20150473, 2015. http://dx.doi.org/10.1098/rspa.2015.0473

[14] D. R. Wilkie, "The relation between force and velocity in human muscle," *The Journal of Physiology*, vol. 110, no. 3-4, pp. 249–280, 1949.

[15] L. Mu and I. Sanders, "Neuromuscular compartments and fiber-type regionalization in the human inferior pharyngeal constrictor muscle," *The Anatomical Record*, vol. 264, no. 4, pp. 367–377, Dec. 2001.

[16] M. P. Harber, P. M. Gallagher, A. R. Creer, K. M. Minchev, and S. W. Trappe, "Single muscle fiber contractile properties during a competitive season in male runners," *American Journal of Physiology-Regulatory, Integrative and Comparative Physiology*, vol. 287, no. 5, May 2004.

[17] S. Trappe, M. Harber, A. Creer, P. Gallagher, D. Slivka, K. Minchev, and D. Whitsett, "Single muscle fiber adaptations with marathon training," *Journal of Applied Physiology*, vol. 101, no. 3, pp. 721–727, Mar. 2006.

[18] J. Finer, R. Simmons, and J. Spudich, "Single myosin molecule mechanics: Picenewton Forces and Nanometer Steps," *Nature*, vol. 10, no. 368, pp. 113–119, Mar. 1994.
[19] M. Casas, P. Llanos, G. Jorquera, J. Hidalgo, S. Buvinic, and E. Jaimovich, "Atp-Induced Membrane Depolarization Relates to Skeletal Muscle Fibers Plasticity," *Biophysical Journal*, vol. 104, no. 2, Apr. 2014.
[20] N. A. Campbell, L. A. Urry, M. L. Cain, S. A. Wasserman, P. V. Minorsky, and J. B. Reece, *Campbell biology in focus*. Harlow, Essex, England: Pearson Education Limited, 2017.